Ultrafast Excited-State Dynamics and Photolysis in Base-Off B_{12} Coenzymes and Analogues: Absence of the trans-Nitrogenous Ligand Opens a Channel for Rapid Nonradiative Decay

Jian Peng, Kuo-Chun Tang, Kaitlin McLoughlin, Yang Yang, Danika Forgach, and Roseanne J. Sension*

Department of Chemistry and Department of Physics, University of Michigan, Ann Arbor, Michigan 48109-1055

Received: May 20, 2010; Revised Manuscript Received: July 12, 2010

Ultrafast transient absorption spectroscopy was used to investigate the photochemistry of adenosylcobalamin (AdoCbl), methylcobalamin (MeCbl), and *n*-propylcobalamin (PrCbl) at pH 2 where the axial nitrogenous ligand is replaced by a water molecule. The evolution of the difference spectrum reveals the internal conversion process and spectral characteristics of the S_1 excited state. The photolysis yield in the base-off cobalamins is controlled by competition between internal conversion and bond homolysis. This is in direct contrast to the process in most base-on alkylcobalamins where primary photolysis occurs with near unit quantum yield and the photolysis yield is controlled by competition between diffusive separation of the radical pair and geminate recombination. The absence of the axial nitrogenous ligand in the base-off cobalamins modifies the electronic structure and opens a channel for fast nonradiative decay. This channel competes effectively with the channel for bond dissociation, dropping the quantum yield for primary radical pair formation from unity in base-on PrCbl and AdoCbl to 0.2 ± 0.1 and 0.12 ± 0.06 in base-off PrCbl and AdoCbl, respectively. The photolysis of base-off MeCbl is similar to that of base-off AdoCbl and PrCbl with competition between rapid nonradiative decay leading to ground state recovery and formation of a radical pair following bond homolysis.

Introduction

Vitamin B_{12} (CNCbl) (Figure 1) is an essential human nutrient, a precursor to the alkylcobalamins incorporated into two human enzymes: methylmalonyl-CoA mutase and methionine synthase.[1−4] Methylcobalamin (MeCbl) functions as a methyl cation donor in methionine synthase and other methyltransferase enzymes.[2] Bond homolysis of the carbon−cobalt bond in 5′-deoxyadenosylcobalamin (coenzyme B_{12}, AdoCbl) functions as a source of organic radicals in cobalamin-dependent enzymes catalyzing radical rearrangement reactions.[1,4] Two major conformations of the B_{12} coenzymes are found in active enzymes: a "base-on" form where the bottom axial ligand to the cobalt is supplied by the dimethylbenzimidazole, as shown in Figure 1, and a "base-off/His-on" conformation in which a histidine residue in the protein provides the axial ligand. A small number of methyltransferase proteins lack an axial nitrogenous ligand, and recent work has demonstrated the presence of a water ligand axial to the methyl.[2,5−7]

In addition to the active B_{12} dependent enzymes, there are transport and transfer proteins that carry the necessary cobalamin cofactors, moving them through the body and preparing the cofactors for the enzymes. One such protein, human adenosyltransferase (ATR), binds cob(II)alamin, adds the 5'-deoxyadenosyl group, and delivers AdoCbl to methylmalonyl-CoA mutase. Recent spectroscopic and structural studies of ATR have demonstrated that this compound binds the cobalamin cofactor in a base-off conformation without an axial nitrogenous ligand in both the cob(III)alamin and cob(II)alamin oxidation states.[8−10] The surprising presence of "base-off" cobalamin in ATR has led to increased interest in the influence of the axial ligand on the active C−Co bond.

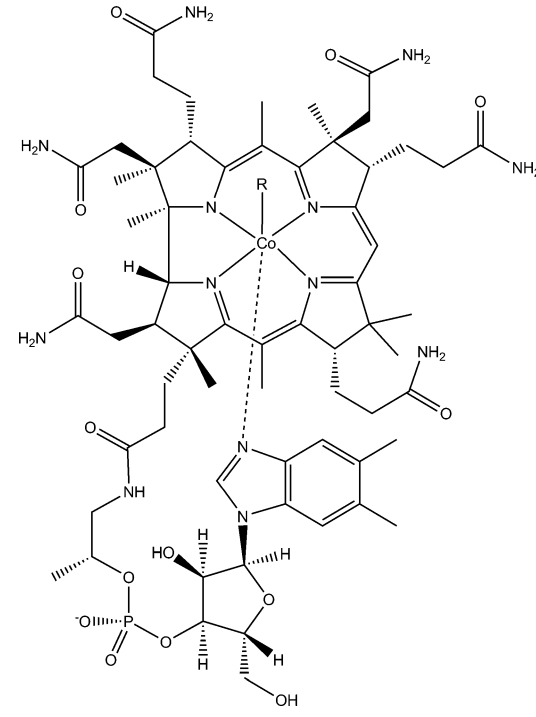

Figure 1. Structure of cobalamins (RCbl). The R group is cyano in vitamin B_{12}, methyl in methylcobalamin, and 5′-deoxyadenosyl in adenosylcobalamin.

The influence of the protein environment and axial ligand in stabilizing or destabilizing the Co−C bond remains a question for investigation. Many spectroscopic and theoretical studies

* To whom correspondence should be addressed. E-mail: rsension@umich.edu.

10.1021/jp104641u
Published on Web 09/03/2010

have sought to understand the relationship between the electronic structure, geometry, and environment of cobalamin cofactors.[11] The cobalamin cofactor is a large molecule with a somewhat flexible ring structure. Density functional theory (DFT) is the method of choice, and time-dependent density functional theory (TDDFT) is required to model the excited state spectrum. Brunold and co-workers have combined TDDFT calculations with extensive spectroscopic measurements to describe the electronic structure of cobalamins in solution and bound to a variety of proteins.[5,10,12−16]

Recent calculations by Kozlowski and co-workers have explored the electronic structure and photochemistry of base-on and base-off cobalamins in detail.[17−21] These calculations highlight some of the difficulties in modeling such a complex molecule; the B3LYP functional appropriate for modeling the $\pi \rightarrow \pi^*$ transitions of the corrin ring is not appropriate for the d/$\pi \rightarrow \pi^*$/d transitions sensitive to the axial ligation of the cobalt. The BP86 functional does a better job of modeling transitions relevant to the reactivity of the cobalt axial ligands. This functional was used to interpret the distinctive photochemistry of MeCbl.[17,20] Similar TDDFT studies of AdoCbl demonstrate an important distinction between simple alkyl ligands and the more complicated 5′-deoxyadenosyl ligand.[18] Ligand-ring charge transfer transitions (LRCT) involving Ado $\rightarrow \pi^*$ transitions are predicted to contribute to the low-lying states. In a solvent-free model with the BP86 functional, the lowest energy transition is a LRCT transition. These transitions shift to higher energy when a polarizable continuum model (PCM) is used to incorporate solvent effects but still fall within the visible region of the spectrum.

Photoexcitation has proven to be a useful technique in the investigation of B_{12} coenzymes both in solution and protein bound.[22−27] These studies provide insight into the electronic structure of cobalamins and provide a means to produce and study the geminate radical pair. We have reported time-resolved studies of the photolysis of both native AdoCbl[28−31] and MeCbl[32,33] coenzymes as well as the ethylcobalamin (EtCbl) and *n*-propylcobalamin (PrCbl) analogues.[34,35] These studies demonstrate that photolysis of AdoCbl is insensitive to excitation wavelength (400 nm vs 520 nm), producing a geminate radical pair within 100−130 ps at room temperature.[28,29,31] The nature of the S_1 excited state from which the radical pair is formed depends on the environment and exhibits different spectral features in water, ethylene glycol, and the glutamate mutase active site.[28,29,35,36] The photolysis of MeCbl is wavelength-dependent with both prompt dissociation and formation of a long-lived S_1 state ($\geq$1 ns) following excitation at 400 nm but only formation of the long-lived S_1 state following excitation at 520 nm.[32,33,36] The spectral features of the excited state are the same in all environments studied: water, ethylene glycol, and methionine synthase.[32,35] Ethyl- and *n*-propylcobalamin form a geminate radical pair within 50 ps following excitation at both 400 and 520 nm. A contribution arising from rapid dissociation is observed following excitation at 400 nm, while a short-lived S_1 state (<50 ps), spectrally similar to that observed following excitation of MeCbl, is more prominent following excitation at 520 nm.[34,35]

Kozlowski and co-workers have applied TD-DFT methods to explore photochemical bond homolysis in MeCbl and EtCbl.[17,20] In accord with the finding that the BP86 functional does a better job of modeling the C−Co bond, this functional was used to study the electronic state manifold along the reaction coordinate. These calculations identify a dissociative $^3(\sigma_{Co-C} \rightarrow \sigma^*_{Co-C})$ state that drops in energy as the C−Co bond lengthens and suggest that this state mediates the bond dissociation. Differences in the depth of the S_1 minimum and location of the $^3(\sigma_{Co-C} \rightarrow \sigma^*_{Co-C})$ crossing influence the observed rate for dissociation. The calculations predict that dissociation will produce a triplet radical pair. In contrast, recent steady state photolysis measurements investigating the magnetic field effect on the recombination of the geminate radical pair suggest that the majority of radical pairs produced following excitation of both AdoCbl and MeCbl are formed in the singlet state.[25] The mechanism for photolysis in B_{12} coenzymes and analogues remains a phenomenon requiring investigation, both computational and experimental.

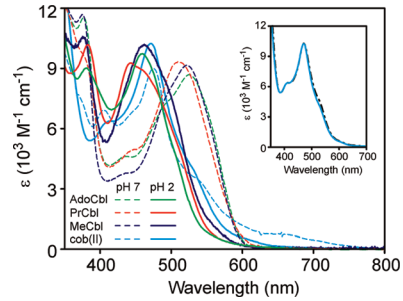

Figure 2. Absorption spectra of adenosylcobalamin (green), propylcobalamin (red), methylcobalamin (dark blue), and cob(II)alamin (light blue). The inset shows the spectrum of cob(II)alamin obtained by photolyzing AdoCbl at pH 7 and then adding acid (dark blue dashed line) and by photolyzing AdoCbl at pH 2 (light blue solid line). The shoulder around 540 nm varies depending on the method used to form cob(II)alamin and may represent the contribution of an oxidation product.

One straightforward way to expand the experimental database of information available is to explore the photochemistry and photophysics of alkylcobalamins in a variety of different states and environments. The presence of "base-off" cobalamin in ATR and corrinoid iron−sulfur proteins has led to increased interest in the electronic structure of this cofactor and suggests that an investigation of base-off cobalamins may contribute to both an understanding of the intrinsic electronic structure of these important coenzymes and to the ways in which the environment can influence the reactivity of the critical C−Co bond. The transition from base-on to base-off can be achieved by lowering the pH of the sample and is characterized by a blue-shift of the dominant absorption feature by ca. 55 nm, from 525 to 459 nm in AdoCbl (Figure 2). A similar blue-shift is observed for MeCbl and other alkylcobalamins. In this paper, we present transient absorption studies of AdoCbl, MeCbl, and PrCbl at pH 2 where the dimethylbenzimidazole base is protonated and the cobalamin is in a base-off configuration.

Experimental Methods

Adenosylcobalamin and methylcobalamin were obtained from Sigma-Aldrich and used without further purification. *n*-Propylcobalamin was synthesized and purified according to literature methods as described previously.[34] The aqueous solutions were prepared and studied under anaerobic conditions at all times. Doubly distilled water was deoxygenated by bubbling nitrogen through it for a minimum of 1 h and added to the solid cobalamin samples immediately prior to the spectroscopic measurements. The sample concentrations used were 0.8 mM for adenosylcobalamin, 2.1 mM for methylcobalamin, and 1.5 mM for *n*-propylcobalamin. To prepare the cobalamins in their base-off form, the solution pH value was adjusted to 2 with the addition of a small volume of deoxygenated HCl (2 M standard

solution, Sigma-Aldrich). A nitrogen atmosphere of positive pressure was maintained above the sample solutions over the course of the experiments to prevent oxygen dissolution. The samples were kept in a reservoir and circulated through a flow cell of 1 mm optical path length (0.5 mm for MeCbl) to refresh the sample volume between laser pulses.

Ultrafast transient absorption measurements with 405−410 nm pump and white light continuum probe were performed using a 1 kHz Ti:sapphire laser system described previously.[36] Briefly, output from a self-mode-locked Ti:sapphire oscillator was amplified with a multipass amplifier and compressed into 70 fs pulses centered at approximately 810−820 nm, with 250 μJ per pulse. A beam splitter was used to reflect 80% of the pulse energy to be frequency doubled in a 500 μm type I β-barium borate (BBO) crystal, generating pump pulses centered at 405−410 nm with 6 μJ per pulse energy. The remaining 20% of the amplified pulse energy was focused into 5 mm of flowing ethylene glycol to generate a visible white light continuum. With a spectrum extending from 400 nm to beyond 800 nm, the white light continuum served as the broadband probe. For the measurement of MeCbl photolysis, the continuum was generated in a translating piece of CaF_2, producing a continuum extending from 340 nm to beyond 800 nm. The probe pulses were delayed with respect to the pump pulses by a computer-controlled motorized translation stage; the maximum delay was 1 ns. The pump and probe beams were focused into a 200 μm spot size and made to overlap inside the sample volume, near their respective beam waists. In all measurements, the polarization of the pump beam was set at magic angle (54.7°) with respect to the polarization of the probe beam to ensure that only isotropic responses were measured. A variable neutral density filter was used to adjust the pump intensity for sample excitation. After passing through the sample, the probe beam was coupled into the entrance slit of a photodiode array spectrometer (BWTEK741E-512, for AdoCbl and PrCbl) or a CCD based spectrometer (AvaSpec-2048-USB2, for MeCbl) with an optical fiber. A 1 mm BG39 Schott glass filter was used to attenuate the excessive near-IR component of the transmitted probe to prevent detector saturation. A mechanical chopper synchronized to the 1 kHz reference was placed in the pump beam and set to operate at 100 Hz, providing five-pulse pump-on/pump-off modulations. Taking the common log of the transmitted probe intensity ratio then gave the difference absorption spectra. A difference absorption spectrum recorded at one delay step was computed from averaging 800 pairs of pump-on/pump-off measurements. The data from four repeated measurements were averaged together to give the frequency resolved transient absorption spectra reported below.

The photochemistry of alkylcobalamins may contain contributions arising from multiphoton excitation of the cofactor. Because the magnitude of the difference spectrum at long times (>200 ps) following excitation of the base-off compounds is quite small (see below), it was important to investigate this power dependence. The variable neutral density filter in the pump arm was used to vary the pump intensity over a factor of 4 from 0.5 to 2 μJ/pulse. The 600 ps scans in base-off AdoCbl exhibit a structured peak at 470 nm with a linear dependence on the pump intensity and a component with approximately cubic intensity dependence and an almost monotonically increasing intensity from 420 to 660 nm. A similar spectral feature, increasing across the visible and peaking at wavelengths longer than 700 nm, is observed following multiphoton excitation of base-on MeCbl at 400 nm. The data reported below for the photolysis of AdoCbl, MeCbl, and PrCbl at pH 2 were obtained at pump intensities where linear excitation dominates the observed transient absorption signal.

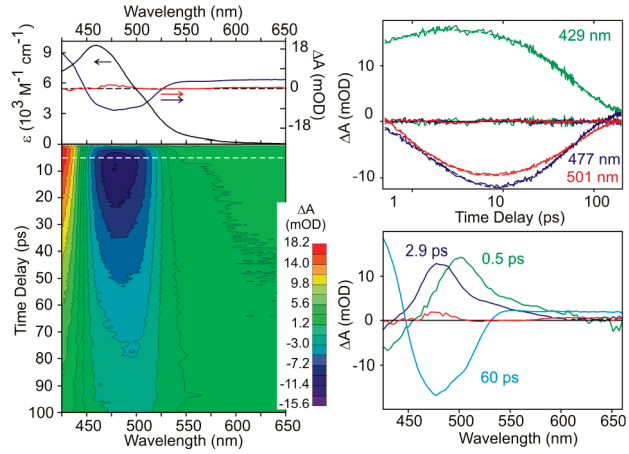

Figure 3. Change in absorption following excitation of AdoCbl at pH 2. Left: The transient spectra at 5 ps (blue) and 600 ps (red) are compared with the steady state spectrum in the top panel. The bottom panel contains a contour plot of the absorption change between 425 and 650 nm over the first 100 ps. Right: The top graph shows sample traces (solid lines) with exponential fits (dashed lines). The residuals are also included in the plot. The bottom graph shows the decay associated difference spectra (DAD spectra) obtained by plotting the amplitude of each exponential decay component as a function of wavelength. The red line is the long-lived component measured at 600 ps, the same as shown in the upper left-hand plot.

The steady state spectrum of base-off cob(II)alamin was measured by photolysis of AdoCbl in the presence of the radical scavenger TEMPO as reported previously,[34,35] followed by addition of acid to drop the pH of the sample. The spectrum was also measured by photolysis of AdoCbl directly at pH 2 in the presence of the radical scavenger. The same product spectrum is obtained by each method, as shown in Figure 2, although the shoulder around 540 nm varies somewhat from scan to scan and may represent the contribution of an oxidation product. UV−visible absorption spectra are reported by Stich et al. for cob(II)inamide prepared by KCOOH reduction of adenosylcobinamide (a cobalamin derivative that lacks the nucleotide loop and the dimethylbenzimidazole base).[15] These spectra are consistent with the possibility that the shoulder around 540 nm represents an oxidation product or incomplete dissociation. The shoulder may also arise from a different conformational placement of the phosphate linkage and dimethylbenzimidazole group absent in the cobinamide.

Results

A. Transient Absorption and Decay Associated Difference Spectra. The transient absorption spectrum of AdoCbl at pH 2 is plotted in Figure 3. Excitation at 400 nm is followed by formation of a deep bleach within a few picoseconds. The broad bleach centered at ca. 480 nm indicates a blue-shift of the excited state spectrum relative to the ground state spectrum. The bleach recovers, leaving a small residual photoproduct spectrum at time delays >200 ps. The data obtained every 3 nm were fit to a sum of three exponential decay components, a fast component of ca. 0.5 ps, and two well-defined components of 2.9 ± 0.24 and 60 ± 3 ps, with a small residual that does not decay on the subnanosecond time scale. Additional components appear to be present at early time, but analysis of the early time behavior is complicated by contributions from coherent two-photon absorption (400 nm + continuum) and by cross-phase modulation within the chirp of the continuum. Sample fits and the decay

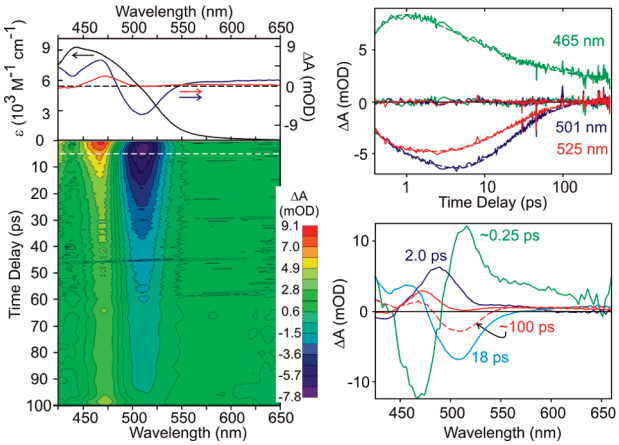

Figure 4. Change in absorption following excitation of PrCbl at pH 2. Left: The transient spectra at 5 ps (blue) and 400 ps (red) are compared with the steady state spectrum in the top panel. The bottom panel contains a contour plot of the absorption change between 425 and 650 nm over the first 100 ps. Right: The top graph shows sample traces (solid lines) with exponential fits (dashed lines). The residuals are also included in the plot. The kinetic traces run to 400 ps. The bottom graph shows the decay associated difference spectra (DAD spectra) obtained by plotting the amplitude of each exponential decay component as a function of wavelength. The solid red line is the long-lived component in the fit to the data.

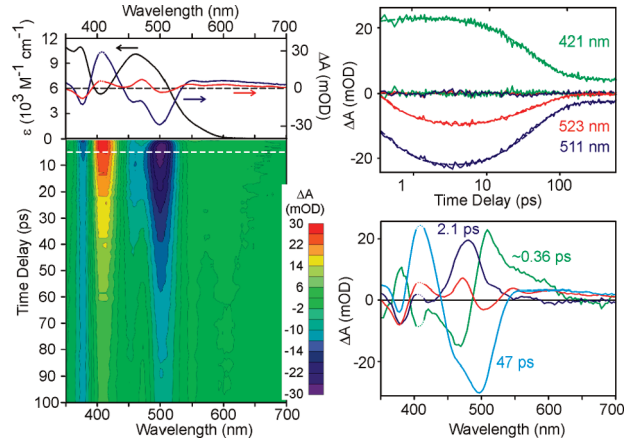

Figure 5. Change in absorption following excitation of MeCbl at pH 2. Left: The transient spectra at 5 ps (blue) and 500 ps (red) are compared with the steady state spectrum in the top panel. The bottom panel contains a contour plot of the absorption change between 425 and 650 nm over the first 100 ps. Right: The top graph shows sample traces (solid lines) with exponential fits (dashed lines). The residuals are also included in the plot. The kinetic traces run to 600 ps. The bottom graph shows the decay associated difference spectra (DAD spectra) obtained by plotting the amplitude of each exponential decay component as a function of wavelength. The solid red line is the long-lived component in the fit to the data.

associated difference spectra (DAD spectra) defined by the amplitudes of each component are plotted in Figure 3.

The transient absorption spectrum obtained following excitation of propylcobalamin is significantly different. There is a net bleaching of the ground state absorption at 510 nm but a net increase in absorption from 425 to 480 nm. The data plotted in Figure 4 were fit to a sum of four exponential decay components, a fast component of ca. 0.25 ps and two well-defined components of 2.0 ± 0.3 and 18 ± 2 ps. A fourth decay component of 100 ± 40 ps was also required by the data. This component has small amplitude, and the precise decay constant is not well-defined by the data; a time constant anywhere from 60 to 150 ps provides a reasonable fit. A small residual signal corresponding to photoproduct does not decay on a subnanosecond time scale. This signal is larger than the corresponding signal observed following excitation of AdoCbl. Sample fits at three wavelengths and the DAD spectra defined by the amplitudes of each component are plotted in Figure 4. The DAD spectra are not affected much by the precise time constant of the ca. 100 ps component. The influence of this rate constant is illustrated in additional plots contained in the Supporting Information.

The transient absorption spectrum obtained following excitation of methylcobalamin is shown in Figure 5. The continuum probe used for this experiment allowed measurement of the transient spectra over a broader wavelength range. There is a net bleaching of the ground state absorption at 500 nm, a net increase in absorption around 410 nm, and a net bleaching again at 375 nm. The data plotted in Figure 5 were fit to a sum of three exponential decay components, a fast component of ca. 0.36 ps, and two well-defined components of 2.1 ± 0.4 and 47 ± 4 ps. The fit to three exponentials provides a good global picture of the dynamics but is not perfect. There is evidence for a small amplitude relaxation component with wavelength dependent rate constant. Sample fits at three wavelengths and the DAD spectra defined by the amplitudes of each component are plotted in Figure 5.

B. Construction of the Species Associated Spectra. The decay associated difference spectra plotted in Figures 3−5

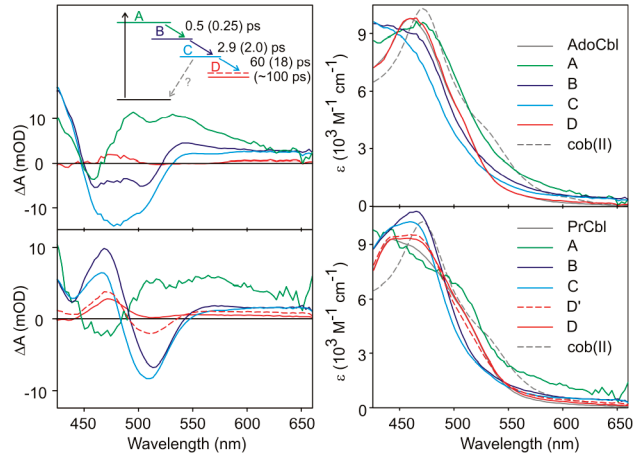

Figure 6. Left: Species associated difference spectra (SAD spectra) calculated for base-off AdoCbl (top) and PrCbl (bottom) following excitation at 400 nm given the model shown in the figure. Lifetimes are shown for AdoCbl (PrCbl). Right: Species associated spectra (SA spectra) calculated from the SAD spectra assuming excitation of 9% of the molecules in the probed volume for AdoCbl and 3% of the molecules in the probed volume for PrCbl.

describe the data but provide little intuitive insight into the nature of the excited electronic states. Species associated spectra provide a better understanding but require a model to interpret the observed spectral changes. The simplest model accounting for the data involves stepwise progression through a series of electronic or conformational states. Excitation results in rapid production of population in an excited state A, the earliest state clearly identified in the data. This population decays on a time scale of 0.25−0.50 ps, proceeding through two distinguishable intermediate states, B and C, to a final state D that persists for times ≫400 ps. An additional state D′ is included for PrCbl, reflecting a relaxation of D or an additional excited electronic state. This scheme is illustrated in Figure 6. The species associated difference spectra (SAD spectra) calculated from the DAD spectra for AdoCbl and PrCbl are plotted in the left-hand panel of Figure 6.

The SAD spectra provide some insight into the nature of the excited state species, but the nature of these states can be seen more clearly in the species associated excited state spectra. The species associated spectra can be reconstructed from the difference spectra given knowledge of the percentage of molecules excited in the probe volume. For AdoCbl at pH 2, the extinction coefficient at 405 nm is 7.4×10^3 M^{-1} cm^{-1}; thus, the absorbance of a 1 mm path length sample of 8×10^{-4} M is 0.59 and 74% of the available photons will be absorbed and 26% will be transmitted. The estimated pulse energy at the sample was 0.9 μJ. At 4.9×10^{-19} J/photon, absorption of 74% of incident photons will yield 1.4×10^{12} excited molecules. The spot size was 0.2 mm in diameter, and the number of molecules in the focal area was 1.5×10^{13}. Thus, the fraction excited is estimated at 1.4/15 = 0.09. Similar calculations for the measurements of PrCbl and MeCbl yield estimates for the excited fraction of 0.03 and 0.075, respectively. These fractions were used to reconstruct the species associated spectra in Figure 6. The reasonable limits for the error in these reconstructions and details for the estimates for PrCbl and MeCbl are presented in the Supporting Information.

The species associated spectra in Figure 6 demonstrate that following excitation at 400 nm AdoCbl exhibits a broad excited state absorption red-shifted from the ground state spectrum. The transition from A to B is correlated with a blue-shift of the excited state absorption on a 0.5 ps time scale. The transition from B to C is correlated with an additional blue-shift of the spectrum. Comparison of the spectra corresponding to states B and C suggests that the 2.9 ps transition represents a relaxation or conformational change in the excited electronic state rather than a transition from one electronic state to another.

The evolution of the excited state spectrum over the first few picoseconds provides a picture of the rapid internal conversion and relaxation of the molecule in the lowest accessible electronic excited state. There is no evidence for intersystem crossing or bond dissociation on this time scale. Thus, the spectrum of state C is assigned to the $S_1 \rightarrow S_n$ transitions of base-off AdoCbl, where the S_1 state is the lowest excited singlet state and S_n represents the manifold of higher-lying excited states accessible from this state. The decay of this excited state on a time scale of 60 ps yields a spectrum nearly identical to the initial ground state spectrum. It is likely that this transition represents a branching between formation of a long-lived product and return to the ground state. The nature of the long-lived photoproduct is discussed in greater detail below.

Excitation of PrCbl results in a broad excited state absorption peaking to the blue of the probe window. This spectrum decays faster than the corresponding species in AdoCbl, and the error in the amplitude is larger. The transition from B to C is accompanied by a blue-shift of the excited state spectrum and a slight decrease in the intensity of the absorption. The spectrum of state C is again assigned to the $S_1 \rightarrow S_n$ transitions from the lowest excited singlet state of base-off PrCbl. The decay of this excited state on a time scale of 18 ps yields a spectrum similar to the initial ground state spectrum. Again, it is likely that the decay of the C state is accompanied by branching between formation of a long-lived photoproduct and return to the ground state. The small amplitude of the long-lived transient makes it difficult to observe changes on a longer time scale for either AdoCbl or PrCbl.

Excitation of MeCbl results in a similar excited state progression (Figure 7), with a broad excited state absorption decaying on a ca. 360 fs time scale to a more structured excited state absorption with peaks around 535 and 466 nm. The transition from B to C on a 2 ps time scale is accompanied by a small decrease in the intensity of the absorption, predominantly the 466 nm peak. The spectrum of state C is assigned to the $S_1 \rightarrow S_n$ transitions of the lowest excited singlet state of base-off MeCbl. The decay of this excited state on a time scale of 47 ps yields a long-lived product with a spectrum peaking at 469 nm. The spectrum of the long-lived photoproduct is stronger than the corresponding transient in AdoCbl or PrCbl.

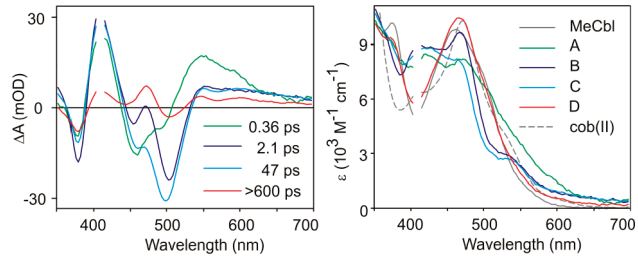

Figure 7. Left: Species associated difference spectra (SAD spectra) calculated for base-off MeCbl following excitation at 410 nm given the model shown in Figure 6. Right: Species associated spectra (SA spectra) calculated from the SAD spectra assuming excitation of 7.5% of the molecules in the probed volume.

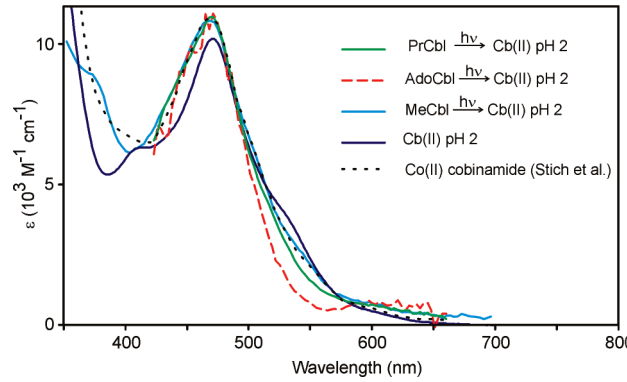

Figure 8. Estimated spectra of the long-lived photoproducts produced following excitation of PrCbl (green solid line, quantum yield = 0.19), AdoCbl (red dashed line, quantum yield = 0.13), and MeCbl (light blue line, quantum yield = 0.65). The cob(II)alamin spectrum measured at pH 2 is shown for comparison. The dotted line represents the room temperature Co(II) cobinamide spectrum reported by Stich et al. in Figure 2 of ref 15.

C. Identification of the Long-Lived Photoproduct as Cob(II)alamin. At pH 2, when the compound is in a base-off conformation, the difference spectrum observed at 400 ps in PrCbl and 600 ps in AdoCbl and MeCbl is characterized by an absorption peak around 470 nm, consistent with formation of a base-off cob(II)alamin. The spectrum of the long-lived photoproduct can be estimated from the data presented above assuming that a similar cob(II)alamin product is formed following excitation of all three compounds. These spectra are plotted in Figure 8. The photolysis product lacks the shoulder at 540 nm observed for base-on and base-off cob(II)alamin produced via room temperature photolysis. However, the spectrum of the product, especially following excitation of PrCbl and MeCbl, is in good agreement with the Co(II) cobinamide spectrum reported by Stich et al.[15] The agreement is quantitative and qualitative; both the shape and the estimated extinction coefficients agree. The spectrum observed following excitation of AdoCbl differs somewhat around 540 nm, but this difference spectrum (see Figure 3) is weak with a relatively small signal-to-noise ratio—the noise is magnified in Figure 8. From these comparisons, we conclude that bond homolysis occurs on a time scale of a few tens of picoseconds.

The estimated quantum yield for bond homolysis is 0.12 ± 0.06 following excitation of AdoCbl and 0.2 ± 0.1 following excitation of PrCbl. In contrast, the estimated quantum yield for bond homolysis in MeCbl is substantially larger at 0.65 (+0.15, −0.25). The error bars reflect uncertainties in the measurements, including the uncertainty in the percentage of molecules excited within the sample volume and uncertainty in the extinction coefficients of the base-off spectra. These quantum yields reflect the primary yield of the radical pair based on the observed difference spectra between 400 and 600 ps. The time scales for diffusive separation of the adenosyl and propyl radicals from the cob(II)alamin in water at 20 °C, pH 7, are 1.6 and 1.5 ns, respectively.[37] Thus, the steady state quantum yield may be influenced by geminate recombination of the radical pair on a time scale longer then the measurements reported here. There is no evidence for geminate recombination in the data, but the signals are small enough that a small amplitude nanosecond recombination cannot be ruled out.

The methyl radical diffuses significantly faster than the larger adenosyl and *n*-propyl radicals. An effective lifetime of 130−400 ps is expected for the contact radical pair based on measurements of recombination in the base-on compound and on simple hydrodynamic calculations.[37] In the data reported here for base-off MeCbl, the transient absorption signal between 200 and 600 ps is constant. Geminate recombination does not occur with any appreciable yield.

These quantum yields can be compared with the quantum yields reported by Taylor et al. for steady state aerobic photolysis of the base-off cobalamins at pH 1.[27] Photolysis of base-off AdoCbl (pH 1) resulted in a homolysis yield of ca. 0.02−0.04 across the spectrum from 250 to 470 nm. This is somewhat lower than the estimate of 0.12 in the current study. Geminate recombination of the radical pair may account for the discrepancy. The photolysis yield following excitation of base-off PrCbl at pH 1 was 0.26 ± 0.02 from 250 to 500 nm, in reasonable agreement with the present measurement at 405 nm. The yield for aerobic homolysis of MeCbl at pH 1 is 0.27 ± 0.02 from 470 to 350 nm, somewhat higher at shorter wavelengths and lower at longer wavelengths. It appears that the primary yield at 600 ps is substantially larger than the steady state quantum yield. Geminate recombination will not account for the discrepancy.

Discussion

The data presented above provide important new insights into the electronic structure and reactivity of alkylcobalamins. The mechanism for bond homolysis is modified by the presence or absence of the nitrogenous axial ligand. The difference in photochemistry reflects the influence of the axial ligand on the electronic structure of the cobalamin and provides additional insight into the role ligation and environment play in the reactivity of the C−Co bond. Accurate electronic structure calculations will be required to fully interpret the observed photochemistry and photophysics of the cobalamin cofactors.

It is also noteworthy that the spectra of the lowest-lying excited states populated following excitation of these three base-off alkylcobalamins are remarkably similar to the spectra of the parent ground state molecules. There is a very weak red absorption tail observed for all three molecules, but the major absorption features begin around 465 nm for both PrCbl and AdoCbl (Figure 6). MeCbl appears to have a smaller band around ca. 530 nm followed by a stronger transition at 465 nm (Figure 7). Early models for the electronic structure of cobalamins assigned the major transitions in the absorption spectrum to $\pi \rightarrow \pi^*$ transitions with vibrational progressions accounting for the shoulders and subpeaks. More recently computational and spectroscopic studies have called this into question, assigning the major features to a complicated manifold of electronic states.[11−21,38] Accurate electronic structure calculations will be able to account for the similarities and differences in the ground and excited state spectra. Thus, these observations provide a constraint for evaluating the calculations.

A. Electronic Structure and Excited State Spectra. Recent TDDFT quantum chemical calculations by Kozlowski and co-workers[18,19] and Brunold and co-workers[5,12] have explored the electronic structure of base-off adenosyl and methyl cobinamides (AdoCbi and MeCbi). Most of these calculations have examined the vertical transitions at the ground state equilibrium geometry. In contrast, the transient absorption experiments probe the excited state spectra as a function of conformational relaxation and at the excited state minimum energy configuration. Nonetheless, it is useful to consider the experimental results in the context of these calculations. Koszlowski and co-workers used B3LYP and BP86 functionals in TDDFT calculations of the electronic transition of MeCbl, MeCbi, AdoCbl, and AdoCbi.[18,19] Calculations of AdoCbl and AdoCbi were also performed using both functionals and a polarizable continuum model to account for the influence of water solvation.[18]

In all of the calculations of base-on and base-off cobalamins, the oscillator strength is carried by transitions involving $\pi \rightarrow \pi^*$ transitions of the corrin ring. The calculations using the B3LYP functional do a better job of handling the $\pi \rightarrow \pi^*$ transitions than the calculations using the BP86 functional. As a result, the B3LYP functional provides a prediction of the absorption spectra. However, the BP86 functional is expected to do a better job of modeling the d/$\pi \rightarrow \pi^*$/d transitions sensitive to the axial ligation of the cobalt.[18,19] Thus, it is useful to consider the results of both methods. All of the calculations for the cobinamides predict one or more states below the $\pi \rightarrow \pi^*$ states responsible for the absorption spectrum.

The B3LYP calculations of MeCbi predict that the lowest singlet state, S_1, contains contributions from the $d_{yz} + \pi$, $d_{xz} + \pi$, and $\pi + d_{yz} \rightarrow \sigma^*_{(Co-C)}$ configurations. The S_2 state contains contributions from the $d_{xz} + \pi \rightarrow \sigma^*$, $\pi + d_y \rightarrow d_{xy} + \pi^*$, and $\pi + d_{z2} \rightarrow \pi^*$ configurations. Both of these states are lower in energy than the dominant $\pi \rightarrow \pi^*$ states carrying the oscillator strength. The calculation using the BP86 functional predicts only one state, with dominant $d_{xy} + \pi \rightarrow \pi^*$ character, below the allowed $\pi \rightarrow \pi^*$ states (Tables S4 and S5 of ref 19). Calculations of AdoCbi show similar trends, with an Ado(π) $\rightarrow \pi^*$ configuration added to the mix (Tables S4 and S5 of ref 18). In fact, the lowest state is dominated by the Ado(π) $\rightarrow \pi^*$ configuration in the calculation using the BP86 functional. When the water solvent is approximated using the PCM model, the Ado(π) $\rightarrow \pi^*$ transitions move to higher energy, although Ado(π^*) mixes with σ^*(Co−C) and contributes to the lowest transitions in the calculation using the B3LYP functional (Tables S11 and S12 of ref 18).

It is dangerous to draw too many conclusions from these calculations. They were performed at the ground state geometry without allowing the excited state geometry to relax. In addition, the methods are not yet well calibrated for the dark states strongly influenced by the Co d atomic orbitals. Nonetheless, it is suggestive that the lowest states are dominated by d orbital excitations. It is also interesting that the σ^*(Co−C) orbital plays a significant role in the lowest transitions, at least in the B3LYP calculations. It appears likely that the excited state spectra of all three base-off compounds resemble the ground state spectra

because the $\pi \rightarrow \pi^*$ transitions are modified only slightly by the change in electronic configuration from the ground to S_1 excited state. In contrast, the lowest state of the base-on cobalamins is an allowed $\pi \rightarrow \pi^*$ state in most of the calculations.[18,19] If the dominant configuration at the minimum energy geometry of the excited state remains the $\pi \rightarrow \pi^*$ configuration, it will explain the more significant differences in excited state spectra for most of the base-on compounds.[36] The observed excited state absorption spectra provide constraints to help validate future electronic structure calculations of alkylcobalamins.

B. Photolysis Mechanism. The photolysis quantum yield in base-off AdoCbl, PrCbl, and MeCbl is dominated by the competition between bond homolysis and fast internal conversion back to the ground state. The data presented above demonstrate that photolysis of these alkylcobalamins results in a rapid cascade through the excited state manifold producing an excited state with a lifetime of 18−60 ps, presumably the S_1 state (B and C in Figures 6 and 7). The population in this state branches between bond homolysis, forming base-off cob(II)alamin and an alkyl radical, and recovery of the ground state alkylcobalamin. The relative stability of base-off cobalamins to photodissociation results from a dominant picosecond channel for ground state recovery. The intrinsic rate constant for nonradiative decay to the ground state is estimated from the observed rate constants and estimated quantum yields at ca. 40−50 ns^{-1} for PrCbl, 13−16 ns^{-1} for AdoCbl, and 4−13 ns^{-1} for MeCbl.

In contrast, the base-on alkylcobalamins exhibit no ground state recovery on a subnanosecond time scale. The photolysis quantum yield in base-on AdoCbl and PrCbl at neutral pH is determined by the competition between primary geminate recombination of the radical pair and diffusive separation of the radicals.[29,34] This geminate recombination behaves as expected as a function of both temperature and solvent viscosity.[37] The only clear evidence for ground state recovery via internal conversion is observed following excitation of methylcobalamin (MeCbl). At room temperature, the excited state decays on a 1 ns time scale with the quantum yield for ground state recovery ∼0.85. Thus, the rate constant for internal conversion is ∼0.85 ns^{-1}. The rate constant for internal conversion in all other alkylcobalamins investigated (ethyl, propyl, adenosyl, and hexylnitrile) is no larger than the rate constant in MeCbl.

Replacement of the bottom nitrogenous axial ligand in MeCbl, PrCbl, and AdoCbl with a water molecule changes the electronic structure and opens a channel for rapid internal conversion. The rate constant for internal conversion increases ∼10-fold in MeCbl and 10−50-fold or more in AdoCbl and PrCbl. The nature of this channel is not clear from the electronic structure calculations performed to date. Elucidation awaits calculations that include the influence of geometry relaxation in the excited state.

Of equal significance, the absence of a prominent geminate recombination component reveals a change in the intrinsic recombination rate for the geminate radical pair. Kozlowski and co-workers reported TDDFT calculations predicting that photolysis of base-on cobalamins is mediated by the presence of a $^3(\sigma_{Co-C} \rightarrow \sigma^*_{Co-C})$ state. This state drops in energy as the C−Co bond length increases. However, production of a triplet radical pair seems inconsistent with the magnetic field effect reported by Jones et al.[25] and is hard to reconcile with the prominent geminate recombination component in the transient absorption data.[37] The magnetic field effect experiments used a broad band white light source for excitation. To test the possible influence of the wavelength-dependent photochemistry of MeCbl, Jones et al. compared measurements carried out with a <400 nm filter and in the absence of the filter. While the photolysis yield reflected the wavelength dependence reported in other studies, the magnetic field effect was unaffected by the filter (Figure S5 of ref 25). From this, it was inferred that the initial radical pair is produced in the singlet state independent of excitation wavelength.

In contrast, the lack of geminate recombination in base-off cobalamins is consistent with the formation of the geminate radical pair in a triplet state, the $^3(\sigma_{Co-C} \rightarrow \sigma^*_{Co-C})$ state, and suggests possibilities for future studies, both experimental and computational.

Finally, another extreme is seen in the base-on cob(III)alamins with nonalkyl ligands. These compounds are photostable because a channel for rapid internal conversion leads to ground state recovery.[39] The lifetime of the excited state is 1−7 ps (rate constant 150−1000 ns^{-1}) in room temperature aqueous solution, with no permanent photoproduct formed. The nature of the axial ligand in these cob(III)alamins opens a channel for internal conversion an order of magnitude faster than the channel in base-off alkylcobalamins. Calculations comparing the photolysis of base-off and base-on cobalamins, and comparing both with the rapid internal conversion in nonalkylcobalamins, may shed new light on the influence of axial ligation on the electronic structure.

Summary and Conclusion

The relative stability of base-off cobalamins to photodissociation arises from a dominant picosecond channel for ground state recovery. The photolysis yield is controlled by competition between internal conversion and bond homolysis. No significant recombination of the geminate radical pair is observed. This is in distinct contrast to the base-on cobalamins where the photolysis yield is controlled to a large extent by competition between geminate recombination and diffusive separation of the geminate radical pair. The nature of the changes in electronic structure of the base-off alkylcobalamins, opening a channel for rapid internal conversion and nonradiative decay and reducing geminate recombination, presents a challenge for quantum chemical simulations of the C−Co bond and will shed light on the mechanism available for the control of the reactivity of this critical enzymatic site.

Acknowledgment. This work is supported in part by the NSF through grant CHE-0718219. Y.Y. was supported by the summer China-USA REU program.

Supporting Information Available: Plots illustrating the influence of the magnitude of the long time constant in the analysis of PrCbl and the limits for acceptable reconstruction of the species associated spectra. The estimates for excitation percentages of PrCbl and MeCbl are worked out. This material is available free of charge via the Internet at http://pubs.acs.org.

References and Notes

(1) Banerjee, R.; Ragsdale, S. W. *Annu. Rev. Biochem.* **2003**, *72*, 209–247.
(2) Matthews, R. G.; Koutmos, M.; Datta, S. *Curr. Opin. Struct. Biol.* **2008**, *18*, 658–666.
(3) Ludwig, M. L.; Matthews, R. G. *Annu. Rev. Biochem.* **1997**, *66*, 269–313.
(4) Marsh, E. N. G. *Essays Biochem.* **1999**, *34*, 139–154.
(5) Stich, T. A.; Seravalli, J.; Venkateshrao, S.; Spiro, T. G.; Ragsdale, S. W.; Brunold, T. C. *J. Am. Chem. Soc.* **2006**, *128*, 5010–5020.

(6) Seravalli, J.; Brown, K. L.; Ragsdale, S. W. *J. Am. Chem. Soc.* **2001**, *123*, 1786–1787.
(7) Ragsdale, S. W.; Lindahl, P. A.; Munck, E. *J. Biol. Chem.* **1987**, *262*, 14289–14297.
(8) Padovani, D.; Banerjee, R. *Biochemistry* **2009**, *48*, 5350–5357.
(9) Yamanishi, M.; Labunska, T.; Banerjee, R. *J. Am. Chem. Soc.* **2005**, *127*, 526–527.
(10) Stich, T. A.; Yamanishi, M.; Banerjee, R.; Brunold, T. C. *J. Am. Chem. Soc.* **2005**, *127*, 7660–7661.
(11) Brunold, T. C.; Conrad, K. S.; Liptak, M. D.; Park, K. *Coord. Chem. Rev.* **2009**, *253*, 779–794.
(12) Stich, T. A.; Brooks, A. J.; Buan, N. R.; Brunold, T. C. *J. Am. Chem. Soc.* **2003**, *125*, 5897–5914.
(13) Stich, T. A.; Buan, N. R.; Escalante-Semerena, J. C.; Brunold, T. C. *J. Am. Chem. Soc.* **2005**, *127*, 8710–8719.
(14) Brooks, A. J.; Fox, C. C.; Marsh, E. N. G.; Vlasie, M.; Banerjee, R.; Brunold, T. C. *Biochemistry* **2005**, *44*, 15167–15181.
(15) Stich, T. A.; Buan, N. R.; Brunold, T. C. *J. Am. Chem. Soc.* **2004**, *126*, 9735–9749.
(16) Brooks, A. J.; Vlasie, M.; Banerjee, R.; Brunold, T. C. *J. Am. Chem. Soc.* **2004**, *126*, 8167–8180.
(17) Lodowski, P.; Jaworska, M.; Andruniow, T.; Kumar, M.; Kozlowski, P. M. *J. Phys. Chem. B* **2009**, *113*, 6898–6909.
(18) Andruniow, T.; Jaworska, M.; Lodowski, P.; Zgierski, M. Z.; Dreos, R.; Randaccio, L.; Kozlowski, P. M. *J. Chem. Phys.* **2009**, *131*.
(19) Andruniów, T.; Jaworska, M.; Lodowski, P.; Zgierski, M. Z.; Dreos, R.; Randaccio, L.; Kozlowski, P. M. *J. Chem. Phys.* **2008**, *129*, 085101.
(20) Jaworska, M.; Lodowski, P.; Andruniow, T.; Kozlowski, P. M. *J. Phys. Chem. B* **2007**, *111*, 2419–2422.
(21) Kuta, J.; Patchkovskii, S.; Zgierski, M. Z.; Kozlowski, P. M. *J. Comput. Chem.* **2006**, *27*, 1429–1437.
(22) Chagovetz, A. M.; Grissom, C. B. *J. Am. Chem. Soc.* **1993**, *115*, 12152–12157.
(23) Grissom, C. B. *Chem. Rev.* **1995**, *95*, 3–24.
(24) Hung, R. R.; Grabowski, J. J. *J. Am. Chem. Soc.* **1999**, *121*, 1359–1364.
(25) Jones, A. R.; Woodward, J. R.; Scrutton, N. S. *J. Am. Chem. Soc.* **2009**, *131*, 17246–17253.
(26) Taoka, S.; Padmakumar, R.; Grissom, C. B.; Banerjee, R. *Bioelectromagnetics* **1997**, *18*, 506–513.
(27) Taylor, R. T.; Smucker, L.; Hanna, M. L.; Gill, J. *Arch. Biochem. Biophys.* **1973**, *156*, 521–533.
(28) Walker, L. A., II; Shiang, J. J.; Anderson, N. A.; Pullen, S. H.; Sension, R. J. *J. Am. Chem. Soc.* **1998**, *120*, 7286–7292.
(29) Yoder, L. M.; Cole, A. G.; Walker, L. A., II; Sension, R. J. *J. Phys. Chem. B* **2001**, *105*, 12180–12188.
(30) Sension, R. J.; Cole, A. G.; Harris, A. D.; Fox, C. C.; Woodbury, N. W.; Lin, S.; Marsh, E. N. G. *J. Am. Chem. Soc.* **2004**, *126*, 1598–1599.
(31) Sension, R. J.; Harris, D. A.; Stickrath, A.; Cole, A. G.; Fox, C. C.; Marsh, E. N. G. *J. Phys. Chem. B* **2005**, *109*, 18146–18152.
(32) Walker, L. A., II; Jarrett, J. T.; Anderson, N. A.; Pullen, S. H.; Matthews, R. G.; Sension, R. J. *J. Am. Chem. Soc.* **1998**, *120*, 3597–3603.
(33) Shiang, J. J.; Walker, L. A., II; Anderson, N. A.; Cole, A. G.; Sension, R. J. *J. Phys. Chem. B* **1999**, *103*, 10532–10539.
(34) Cole, A. G.; Yoder, L. M.; Shiang, J. J.; Anderson, N. A.; Walker, L. A., II; Banaszak Holl, M. M.; Sension, R. J. *J. Am. Chem. Soc.* **2002**, *124*, 434–441.
(35) Sension, R. J.; Harris, D. A.; Cole, A. G. *J. Phys. Chem. B* **2005**, *109*, 21954–21962.
(36) Harris, D. A.; Stickrath, A. B.; Carroll, E. C.; Sension, R. J. *J. Am. Chem. Soc.* **2007**, *129*, 7578–7585.
(37) Stickrath, A.; Carroll, E. C.; Dai, X.; Harris, D. A.; Rury, A.; Smith, B.; Tang, K.-C.; Wert, J.; Sension, R. J. *J. Phys. Chem. A* **2009**, *113*, 8513–8522.
(38) Kozlowski, P. M.; Andruniow, T.; Jarzecki, A. A.; Zgierski, M. Z.; Spiro, T. G. *Inorg. Chem.* **2006**, *45*, 5585–5590.
(39) Shiang, J. J.; Cole, A. G.; Sension, R. J.; Hang, K.; Weng, Y.; Trommel, J. S.; Marzilli, L. G.; Lian, T. *J. Am. Chem. Soc.* **2006**, *128*, 801–808.

JP104641U